Table IV. Crystal and Intensity Collection Data

formula	$C_{24}H_{41}N_6BOZn$	Z	3
fw	505.8	space group	$R3m$ (No. 160)
lattice	rhombohedral	radiation (λ, Å)	Mo Kα (0.71073)
cell consts	$a = 15.995$ (2) Å		
	$b = 15.995$ (2) Å	ρ_{calcd}	1.21 g cm^{-3}
	$c = 9.391$ (2) Å	μ(Mo Kα)	9.4 cm^{-1}
	$\alpha = 90.0°$	goodness of fit	1.073
	$\beta = 90.0°$	R	0.0385
	$\gamma = 120.0°$	R_w[a]	0.0369
	$V = 2080.5$ (7) Å^3		

[a] Weighting scheme: $w = [\sigma^2(F) + 0.0002F^2]^{-1}$

zyme–Zn–OCO_3H] complex has a distorted 5-fold coordination (see Scheme I).[10] For both these geometries we have now found small-molecule equivalents in the form of [tris(pyrazolyl)hydroborato]zinc complexes, namely the hydroxide $\{\eta^3$-HB(3-Bu^t-5-Mepz)$_3\}$ZnOH with pseudotetrahedral coordination and the nitrate $\{\eta^3$-HB(3-Phpz)$_3\}$Zn(η^2-NO_3) with distorted 5-fold coordination.[5c] The new hydroxide complex $\{\eta^3$-HB(3-Bu^t-5-Mepz)$_3\}$ZnOH also seems to be promising with respect to the mechanism of carbonic anhydrase activity. Thus, we have observed that solutions of $\{\eta^3$-HB(3-Bu^t-5-Mepz)$_3\}$ZnOH do indeed reversibly absorb CO_2, giving a compound that shows two absorptions at 1675 and 1302 cm^{-1}, which may be assigned to the bicarbonate complex $\{\eta^3$-HB(3-Bu^t-5-Mepz)$_3\}$Zn(OCO_2H).[12] The bicarbonate complex undergoes subsequent reaction to give the bridging carbonate complex [$\{\eta^3$-HB(3-Bu^t-5-Mepz)$_3\}$Zn]$_2$(μ_2-OC(O)O),[13] in a manner analogous to that observed for the reaction of the dinuclear copper hydroxide complex [$\{\eta^3$-HB(3,5-Pr$^i_2$pz)$_3\}$Cu(μ-OH)]$_2$ to give [$\{\eta^3$-HB(3,5-Pr$^i_2$pz)$_3\}$Cu]$_2$(μ_3-CO_3)].[14]

Experimental Section

General Considerations. NMR spectra were recorded on a Bruker AC 200 FL spectrometer, and IR spectra were recorded as Nujol mulls on a Bruker IFS 25 spectrophotometer. Details of the preparation of $\{$HB-(3-Bu^t-5-Mepz)$_3\}$K will be published elsewhere.[15]

Preparation of $\{\eta^3$-HB(3-Bu^t-5-Mepz)$_3\}$ZnOH. Zn(ClO_4)$_2$·6H_2O (205 mg, 0.55 mmol) was added to a solution of $\{$HB(3-Bu^t-5-Mepz)$_3\}$K (250 mg, 0.55 mmol) in methanol (40 mL). After 15 min, a solution of KOH (31 mg, 0.55 mmol) in methanol (10 mL) was added, and the mixture was stirred for 1 h at room temperature. The solution was filtered to remove the precipitate of $KClO_4$, and the filtrate was concentrated in vacuo at room temperature until $\{\eta^3$-HB(3-Bu^t-5-Mepz)$_3\}$ZnOH began to crystallize. Crystallization was completed by cooling to −20 °C for 24 h. The colorless crystals of analytically pure $\{\eta^3$-HB(3-Bu^t-5-Mepz)$_3\}$ZnOH (180 mg, 65%) were collected and dried under vacuum. IR (Nujol mull, cm^{-1}): $\nu_{OH} = 3676$ (w), $\nu_{BH} = 2543$ (m), 2521 (w). ^{1}H NMR (C_6D_6): δ 5.64 (s, 3 H, 3 CH), 2.10 (s, 9 H, 3 CH_3), 1.54 (s, 27 H, 3 C_4H_9), −0.07 (s, 1 H, Zn–OH).[16] ^{13}C NMR ($CDCl_3$): δ 162.8 (3 C, 3 pyrazole C=N), 143.9 (3 C, 3 pyrazole C=N), 102.3 (3 C, 3 pyrazole CH), 31.5 (3 C, 3 $C(CH_3)_3$), 30.3 (9 C, 3 $C(CH_3)_3$), 12.9 (3 C, 3 CH_3). Anal. Calcd for $C_{24}H_{41}BN_6OZn$: C, 56.99; H, 8.17; N, 16.62. Found: C, 56.70; H, 8.10; N, 16.42.

X-ray Structure Determination of $\{\eta^3$-HB(3-Bu^t-5-Mepz)$_3\}$ZnOH. Crystal data and data collection and refinement parameters are summarized in Table IV. A single crystal of $\{\eta^3$-HB(3-Bu^t-5-Mepz)$_3\}$ZnOH was mounted in a glass capillary and placed on a Nicolet R3m diffractometer. The unit cell was determined by the automatic indexing of 25 centered reflections and confirmed by examination of the axial photographs. Intensity data were collected by using graphite-monochromated Mo Kα X-radiation ($\lambda = 0.71073$ Å). Check reflections were measured every 100 reflections, and the data were scaled accordingly and corrected for Lorentz, polarization, and absorption effects. The structure was solved by using direct methods and standard difference map techniques on a Data General NOVA 4 computer using SHELXTL.[17] Systematic absences were consistent with the space groups $R3$, $R\bar{3}$, $R32$, $R3m$, and $R\bar{3}m$, but consideration of the E value statistics, the axial photographs (a and b axes mirror symmetry), and the molecular symmetry strongly suggested the choice $R3m$ (No. 160). Most of the hydrogen atoms were located in the difference map after all the non-hydrogen atoms were located and refined anisotropically, but hydrogens on carbon were allowed to refine in calculated positions ($d_{C-H} = 0.96$ Å; $U_{iso}(H) = 1.2U_{iso}(C)$). Block-diagonal least-squares refinement converged to $R = 0.0385$ ($R_w = 0.0369$). Inversion of configuration indicated the correct choice of enantiomorph. Atomic coordinates and thermal parameters for non-hydrogen atoms are listed in Table I, and selected bond distances and angles are listed in Tables II and III.

Conclusion

The synthesis and structure determination of the zinc hydroxide complex $\{\eta^3$-HB(3-Bu^t-5-Mepz)$_3\}$ZnOH have provided the first mononuclear molecular analogue of the active center of the enzyme carbonic anhydrase, which also offers potential with respect to reactivity studies.

Acknowledgment. This work was supported by the Fonds der Chemischen Industrie, the Deutsche Forschungsgemeinschaft (Grant Va 29/13), and the National Science Foundation Grant CHE-9007512). We thank two of the reviewers for valuable comments. G.P. is the recipient of an A. P. Sloan Research Fellowship (1991–1993) and a Camille and Henry Dreyfus Teacher-Scholar Award (1991–1996).

Supplementary Material Available: Tables SI–SVI, listing crystal and intensity collection data, atomic coordinates, bond distances and angles, and anisotropic displacement parameters for $\{\eta^3$-HB(3-Bu^t-5-Mepz)$_3\}$-ZnOH (4 pages); a listing of calculated and observed structure factors (3 pages). Ordering information is given on any current masthead page.

---

(12) For IR data on bicarbonates see: Nakamoto, K. *Infrared and Raman Spectra of Inorganic and Coordination Compounds*, 4th ed.; Wiley-Interscience: New York, 1986.

(13) [$\{\eta^3$-HB(3-Bu^t-5-Mepz)$_3\}$Zn]$_2$(μ_2-OC(O)O) has been structurally characterized by single-crystal X-ray diffraction: Looney, A.; Parkin, G. Unpublished results.

(14) Kitajima, N.; Fujisawa, K.; Koda, T.; Hikichi, S.; Moro-oka, Y. *J. Chem. Soc., Chem. Commun.* **1990**, 1357.

(15) Trofimenko, S. Manuscript in preparation.

(16) The assignment of Zn–OH was confirmed by ^{2}H NMR spectroscopy on the deuterium-labeled derivative, $\{\eta^3$-HB(3-Bu^t-5-Mepz)$_3\}$ZnOD.

(17) Sheldrick, G. M. SHELXTL: An Integrated System for Solving, Refining and Displaying Crystal Structures from Diffraction Data. University of Göttingen, Göttingen, Germany, 1981.

Contribution from the Departments of Chemistry,
Brown University, Providence, Rhode Island 02912,
and University of Vermont, Burlington, Vermont 05405

Palladium(I) π Complexes: An ESR Study of (Pentaphenylcyclopentadienyl)palladium Dibenzocyclooctatetraene

Janice A. DeGray,† William E. Geiger,*,‡ Gregg A. Lane,‡ and Philip H. Rieger*,†

Received March 28, 1991

Paramagnetic Pd π complexes are extremely rare. The most stable such complexes prepared to date are those of the type Cp*Pd(dien), where Cp* = η^5-C_5Ph_5 and dien = a cyclic diolefin such as 1,5-cyclooctadiene.[1] The Pd(I) compounds were generated by electrochemical reduction of the cationic Pd(II) precursors. Analogous Ni(I) complexes are also known.[2] Since knowledge of the half-filled orbital (SOMO) is of obvious relevance to the properties of this class of compound, we thought it would be useful to study a representative member by electron spin resonance (ESR) spectroscopy. The spin-$^5/_2$ ^{105}Pd nucleus is 22.2% in natural abundance, so that palladium nuclear hyperfine structure was expected in the ESR spectrum. Spin density information is carried by the metal nuclear hyperfine coupling tensor.

The pentaphenylcyclopentadienyl complex Cp*Pd(η^4-dbcot) (**1**), dbcot = dibenzocyclooctatetraene, was chosen for this purpose because of the high degree of stability imparted by the dbcot ligand.[1] An additional aspect of this choice was the conformational stability of the dbcot ligand. The aromatic rings have the effect

---

† Brown University.
‡ University of Vermont.

0020-1669/91/1330-4100$02.50/0

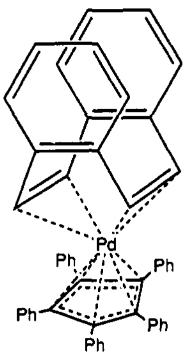

1

of forcing the metal-to-diolefin bonding to occur through nonadjacent double bonds, locking the ligand into a 1,5-bonding mode and minimizing chances for isomerization to a 1,3-diolefin in the Pd(I) oxidation state. The isomerization of similar cobalt(0) diolefins has been discussed.[3]

The results indicate that the SOMO is analogous to that found for isoelectronic d^9 complexes of Co and Rh,[4,5] having roughly equal contributions from both ligand and metal orbitals. The metal contribution is mostly 4d$_{yz}$, although there appears to be a significant admixture of Pd 5p$_y$.

Experimental Section

[Cp*Pd(η^4-dbcot)][PF$_6$] (1^+PF$_6^-$) was prepared as previously described.[1] One-electron reduction of 1^+PF$_6^-$ ($E°$ = −0.22 V vs SCE), 10 mM in tetrahydrofuran (THF) solution, was carried out in an electrolysis cell mounted in the ESR cavity. THF was vacuum-distilled from sodium benzophenone ketyl, and the solution contained 0.1 M tetra-*n*-butylammonium perchlorate as a supporting electrolyte. ESR spectra were obtained with a Bruker ER220D spectrometer, equipped with a Systron-Donner 6246A microwave frequency counter, a Bruker ER4111 variable-temperature unit, and an Aspect 2000 computer. Details of the experimental procedure are given elsewhere.[6]

Results and Discussion

ESR Spectra. The isotropic ESR spectrum of **1** at 290 K, shown in Figure 1, consists of a single line, due to the Pd isotopes with zero spin, and four satellites, the $\pm^5/_2$ and $\pm^3/_2$ hyperfine lines of the ^{105}Pd sextet. The *g* value and palladium hyperfine coupling constant are easily measured and are given in Table I. The line width increased at lower temperatures, and in spectra recorded at 190 and 240 K, the ^{105}Pd satellites were not detectable.

The spectrum of **1** in frozen THF at 130 K is shown in Figure 2a. Three major features are observed which can be assigned to the principal values of the **g** tensor. The high-field feature has well-resolved ^{105}Pd satellites with ca. 19-G spacings, and the low-field feature has barely detectable satellites with ca. 36-G spacings.[7] Least-squares analysis[8] of the positions of the satellites, assuming that the principal axes of **g** and **A** are coincident, gave the parameters labeled A_x and A_z shown in Table I. Assuming that $\langle A\rangle$, A_y, and A_z have the same sign, the missing component, A_y, can be estimated from the isotropic coupling and the relation

$$3\langle A\rangle = A_x + A_y + A_z \tag{1}$$

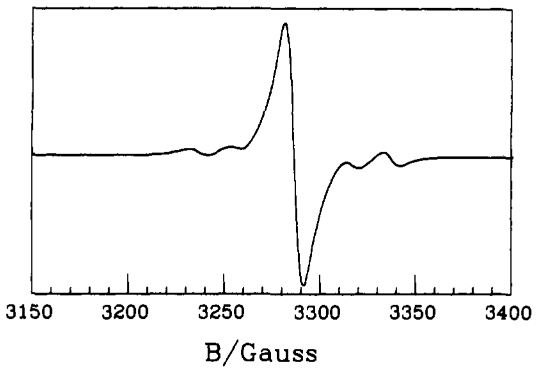

Figure 1. ESR spectrum of **1** in THF at 290 K.

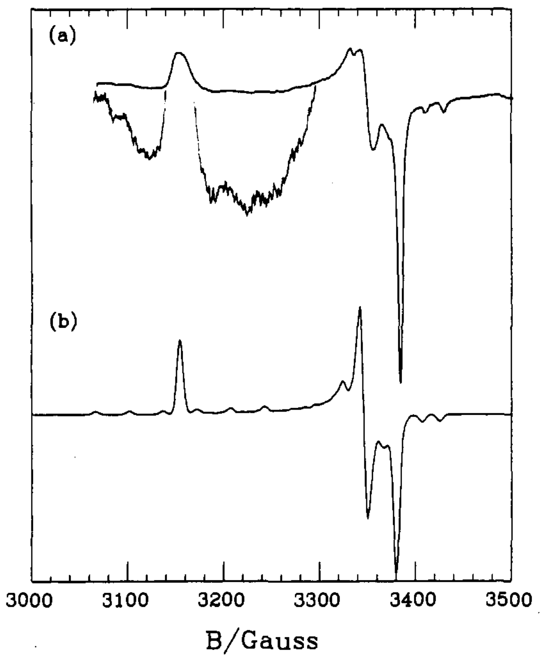

Figure 2. (a) ESR spectrum of **1** in frozen THF at 130 K (inset: gain × 10) and (b) computer simulation using the parameters of Table I.

Table I. ESR Parameters for Cp*Pd(η^4-dbcot) in THF Solutions

direction	g^a	$A^{\mathrm{Pd}}/10^{-4}$ cm^{-1}	direction	g^a	$A^{\mathrm{Pd}}/10^{-4}$ cm^{-1}
isotropic	2.058	(+)19.5 ± 0.3	*y*	2.022	(+)6.1 ± 1.6^b
x	2.145	(+)35.2 ± 1.5	*z*	2.001	(+)17.1 ± 0.3

^{a}Estimated accuracy ± 0.001. ^{b}Computed from $\langle A\rangle$, A_y, and A_z; see text.

If the signs were not the same, the predicted value of A_y would be much larger in magnitude, and satellites should have been resolved around the central feature in the experimental spectrum. A computer-simulated spectrum, based on the parameters of Table I, is shown in Figure 2b.[9]

Interpretation of ESR Parameters. If we regard **1** as having approximate C_{2v} symmetry with the molecular *z* axis directed through the center of the Cp* ring and the coordinated double bonds of the dbcot ligand centered on the *yz* plane, MO theory considerations[4,5] suggest that, for a d^9 configuration, the semioccupied molecular orbital (SOMO) is of b$_2$ symmetry with 4d$_{yz}$ and 5p$_y$ contributions

$$|\mathrm{SOMO}\rangle = a|yz\rangle + b|y\rangle + \dots \tag{2}$$

In this case, the **g**-tensor components are expected to be[4]

---

(1) (a) Broadley, K.; Lane, G. A.; Connelly, N. G.; Geiger, W. E. *J. Am. Chem. Soc.* **1983**, *105*, 2486. (b) Lane, G. A.; Geiger, W. E.; Connelly, N. G. *J. Am. Chem. Soc.* **1987**, *109*, 402.

(2) (a) Lane, G. A.; Geiger, W. E. *Organometallics* **1982**, *1*, 401. (b) Koelle, U.; Wesner, H. *J. Organomet. Chem.* **1981**, *221*, 367.

(3) See leading references in: Geiger, W. E.; Gennett, T.; Grzeszczuk, M.; Lane, G. A.; Moraczewski, J.; Salzer, A.; Smith, D. E. *J. Am. Chem. Soc.* **1986**, *108*, 7454.

(4) Connelly, N. G.; Geiger, W. E.; Lane, G. A.; Raven, S. J.; Rieger, P. H. *J. Am. Chem. Soc.* **1986**, *108*, 6219.

(5) (a) Albright, T. A.; Geiger, W. E.; Moraczweski, J.; Tulyathan, B. *J. Am. Chem. Soc.* **1981**, *103*, 4787. (b) Rieger, P. H. In *Organometallic Radical Processes*; Trogler, W., Ed.; Elsevier: Amsterdam, 1990; p 270.

(6) DeGray, J. A. Ph.D. Thesis, Brown University, 1987.

(7) These satellites are not easily seen in the spectrum shown in Figure 2a but are clearly present on magnification. The experimental spectrum does not include the lowest field satellite; the existence of these features was not recognized at the time the spectrum was recorded.

(8) DeGray, J. A.; Rieger, P. H. *Bull. Magn. Reson.* **1987**, *8*, 95.

(9) The computer simulation employed Gaussian line shapes with a constant 3-G width; the widths of the *x* and *y* components of the experimental spectrum are clearly much broader, and the *z* component is somewhat sharper.

$$g_x = g_e + 2a^2(\delta_{x^2-y^2} + 3\delta_{z^2}) + 2b^2\delta_z \qquad (3a)$$

$$g_y = g_e + 2a^2\delta_{xy} \qquad (3b)$$

$$g_z = g_e + 2a^2\delta_{xz} + 2b^2\delta_x \qquad (3c)$$

where the δ_i values are

$$\delta_i = \sum_{k\neq 0}\frac{\lambda_i c_{ik}{}^2}{E_0 - E_k} \qquad (4)$$

In eq 4, λ_i is the spin-orbit coupling parameter for palladium 4d (λ_d) or 5p (λ_p) electrons, c_{ik} is the LCAO coefficient of the ith AO in the kth MO, and $E_0 - E_k$ is the energy difference between the SOMO and the kth MO. The hyperfine components can be written

$$A_x = A_s + P_d a^2[-4/7 + 2(\delta_{x^2-y^2} + 3\delta_{z^2}) + 3/7(\delta_{xy} + \delta_{xy})] + P_p b^2(-2/5 + 2\delta_z + 3/5\delta_x) \qquad (5a)$$

$$A_y = A_s + P_d a^2[2/7 + 2\delta_{xy} - 3/7(\delta_{xz} + \delta_{z^2} - \delta_{x^2-y^2})] + P_p b^2[4/5 - 3/5(\delta_x + \delta_z)] \qquad (5b)$$

$$A_z = A_s + P_d a^2[2/7 + 2\delta_{xz} - 3/7(\delta_{xy} - \delta_{z^2} + \delta_{x^2-y^2})] + P_p b^2(-2/5 + 2\delta_x + 3/5\delta_z) \qquad (5c)$$

where A_s is the isotropic Fermi contact interaction contribution and P_d and P_p are the electron-nuclear dipolar coupling parameters for palladium 4d and 5p electrons. If we neglect the 5p contribution, subtracting the average of eqs 5a-c from eq 5a gives

$$A_x - \langle A\rangle = P_d[-4/7a^2 + 2/3\Delta g_x - 5/42(\Delta g_y + \Delta g_z)] \qquad (6)$$

Substituting experimental values of A_x, $\langle A\rangle$, the Δg_i values, and $P = -62.7 \times 10^{-4}$ cm^{-1} for ^{105}Pd,[10] gives $a^2 = \rho_d = 0.60 \pm 0.04$, where the uncertainty is based on the experimental error in the measurement of A_x. This value can be compared with 3d spin densities of 0.68, 0.59, and 0.53 estimated in the same way for $[CpCo(\eta^4\text{-1,5-COD})]^-$, $[CpCo(\eta^4\text{-1,3-COD})]^-$, and $[CpCo(\eta^4\text{-tpc})]^-$,[11] respectively. Thus, at this level of approximation, the SOMO of the d^9 Pd(I) radical is remarkably similar to those of the isoelectronic Co(0) species. The similarity extends to the **g** tensors, which are (2.171, 2.027, 1.985), (2.151, 2.027, 1.997), and (2.103, 2.025, 1.906) for the three Co(0) radical anions. This similarity is in part fortuitous, since the spin-orbit coupling parameter λ_d is surely larger for Pd; nonetheless, the results suggest a qualitatively similar MO energy level scheme for d^9 complexes of the type CpM(diene).

Just as in our previous work with the $CpCo(CO)_2$ anions,[4] the departure from axial symmetry cannot be rationalized in terms of d-orbital contributions alone. Subtracting eqs 5b and 5c, we have

$$A_y - A_z = P_d a^2[17/7(\delta_{xy} - \delta_{xz}) - 6/7(\delta_{z^2} - \delta_{x^2-y^2})] + P_p b^2(1 - 13/6\delta_x - \delta_z)$$

If we neglect the 5p contributions and assume that the first term dominates, we have

$$A_y - A_z = 17/14 P_d(\Delta g_y - \Delta g_z) = -1.6 \times 10^{-4}\ \text{cm}^{-1}$$

which is much smaller than the observed value, -11×10^{-4} cm^{-1}. The most likely explanation for this discrepancy is the presence of significant 5p$_y$ character in the SOMO.

Tyler[12] has recently distinguished among three classes of 19-electron complexes: (1) complexes in which the 19th electron occupies a metal-ligand σ^* orbital; (2) complexes in which the electron count is lowered by a change in ligand geometry, e.g., a "slipped" η^3-Cp ring; (3) complexes in which the odd electron occupies a ligand π^* orbital—really an 18-electron complex with a radical-anion ligand. ESR spectra can usually distinguish between class 3 and class 1 or 2 complexes, since the g value should be close to the free-electron value and the metal hyperfine coupling should be unusually small in class 3 complexes, e.g., $Co(CO)_3L_2$ [L_2 = 2,3-bis(diphenylphosphino)maleic anhydride], where $\langle g\rangle = 2.004$ and $\langle A^{Co}\rangle = 1.05$ G.[12-14] Distinguishing between class 1 and class 2 complexes by using ESR data is more difficult, since a substantial metal spin density is expected in either case.

Finally, we note that the high degree of covalency found for **1** is consistent with its reaction chemistry. Lane et al.[1b] have shown that this complex and its analogues undergo radical reactions with H, OH, and OR donors through addition to one of the double bonds coordinated to the Pd(I) atom. The observed ligand-based addition reactions are consistent with a significant amount of radical character in the coordinated diolefin.

Acknowledgment. We gratefully acknowledge the support of this research by the National Science Foundation (Grant CHE 86-03728). We also thank Johnson Matthey Co. for a generous loan of palladium acetate.

---

(10) Morton, J. S.; Preston, K. F. *J. Magn. Reson.* **1978**, *30*, 577.

(11) COD = cyclooctadiene; tpc = tetraphenylcyclopentadieneone. These values are obtained by using eqs 5 and the data in ref 5a and: van Willigen, H.; Geiger, W. E.; Rausch, M. D. *Inorg. Chem.* **1977**, *16*, 581.

(12) Mao, F.; Tyler, D. R.; Keszler, D. *J. Am. Chem. Soc.* **1989**, *111*, 130.

(13) Fenske, D. *Chem. Ber.* **1979**, *112*, 363.

(14) Mao, F.; Tyler, D. R.; Rieger, A. L.; Rieger, P. H. *J. Chem. Soc., Faraday Trans.*, in press.